European Journal of Medicinal Chemistry 108 (2016) 21–27

Contents lists available at ScienceDirect

European Journal of Medicinal Chemistry

journal homepage: http://www.elsevier.com/locate/ejmech

Research paper

Novel leucine ureido derivatives as aminopeptidase N inhibitors. Design, synthesis and activity evaluation

Chunhua Ma [a, b], Jiangying Cao [b], Xuewu Liang [b], Yongxue Huang [b], Ping Wu [a], Yingxia Li [a], Wenfang Xu [b], Yingjie Zhang [b, *]

[a] School of Pharmacy, Fudan University, 826 Zhangheng Road, Shanghai 201203, China
[b] School of Pharmaceutical Sciences, Shandong University, Jinan 250012, China

ARTICLE INFO

Article history:
Received 11 July 2015
Received in revised form
11 November 2015
Accepted 14 November 2015
Available online xxx

Keywords:
Aminopeptidase N
Inhibitors
Leucine ureido derivatives
Synthesis

ABSTRACT

Aminopeptidase N (APN/CD13) over-expressed on tumor cells and tumor microenvironment, plays critical roles in tumor invasion, metastasis and angiogenesis. Here we described the design, synthesis and preliminary activity studies of novel leucine ureido derivatives as aminopeptidase N (APN/CD13) inhibitors. The results showed that compound **7a** had the most potent inhibitory activity against APN with the $\mathbf{IC_{50}}$ value of 20 nM, which could be used for further anticancer agent research.

1. Introduction

Aminopeptidase N (APN, also known as CD13; EC 3.4.11.2) is a zinc-dependent type II membrane-bond ectopeptidase that preferentially releases neutral and basic amino acids from the N-terminus of oligopeptides. It has been identified as a cell surface marker for malignant myeloid cells [1] and was over-expressed on various mammalian tumor cells [2], such as melanoma, prostate, ovarian, colon, renal and pancreas carcinomas, as well as tumor microenvironment [3]. APN degrades extracellular matrix (ECM) which is the main barrier of malignant cell dissemination to promote tumor invasion and metastasis [4]. More and more researches indicate that APN is an important angiogenic factor and can serve as a target for delivering drugs into tumors and inhibiting angiogenesis [3,5]. Moreover, APN is a mark and therapeutic target in human liver cancer stem cells which are responsible for tumor resistance to chemo/radiation therapy as well as tumor relapse and progression [6–8]. Accordingly, APN is considered as an important target for anti-tumor research. Therefore, the design and synthesis of APN inhibitors may have clinical significance for the discovery of anticancer agents.

To date, many natural or synthetic small APN inhibitors have been reported. Natural APN inhibitors include Bestatin [9], Probestin [10], AHPA-Val [11], Lapstatin [12], Amastatin [13], *etc.* Synthetic small APN inhibitors include α-aminoaldehydes [14], α-aminophosphiric acids [15], α-aminoboronic acids [16], L-lysine derivatives [17], L-arginine derivatives [18], cyclic-imide derivatives [19,20], β-dicarbonyl derivatives [21] and so on. However, Bestatin is the only marketed APN inhibitor. Low inhibitory activity is the obstruction of APN inhibitors development. So it is necessary to exploit more active APN inhibitors by rational drug design.

In our previous work, we have reported a series of ureido derivatives [22]. The biological characterization revealed that some compounds displayed potential inhibitory activity against APN. Especially, the IC_{50} value of compound **4k** was 2.7 μM compared with 9.1 μM of Bestatin. Herein, in order to find better APN inhibitors, Compound **4k** was used as the lead compound. In our series of L-arginine derivatives, we found that compounds containing disubstituted groups on phenyl had better activities than those containing unsubstituted or single substitution [18]. The same tendency exists in our L-lysine derivatives [17]. Based on these observations, a series of novel leucine ureido derivatives (**7a**–**7k**) containing different disubstitution on the phenyl group of **4k** have been synthesized, meanwhile, some analogues (**8a**–**8g**) with disubstituted benzyl groups replaced the phenyl group of **4k** have also been obtained (Fig. 1). The *in vitro* inhibitory activity was

* Corresponding author.
E-mail address: zhangyingjie@sdu.edu.cn (Y. Zhang).

http://dx.doi.org/10.1016/j.ejmech.2015.11.021
0223-5234/

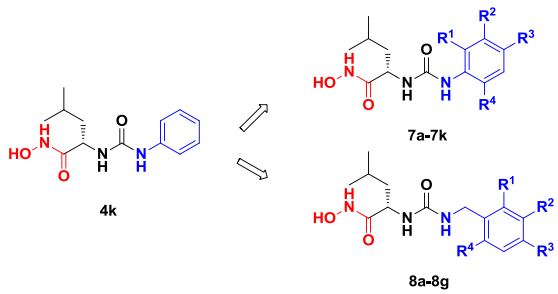

Fig. 1. The new APNIs derived from compound **4k** (two of R are H).

measured against APN enzyme. Additionally, the antimetastasis effect of potent compounds was evaluated *in vitro* and *in vivo* assay.

2. Chemistry

The target compounds were synthesized efficiently via the route outlined in Scheme 1. Starting from commercially available L-leucine, the key intermediate leucine isocyanate was obtained via esterification and isocyanate, and then coupled with the corresponding disubstituted anilines or benzylamines. Without further purification, they were directly transformed into hydroxamic acids as the target products.

3. Result and discussion

The target compounds were evaluated for their inhibitory activities toward **APN** and **HDACs** by the spectrophotometric method as described previously [23,24]. Similar to **APN**, **HDACs** are zinc-dependent metalloproteinases as well and associated closely with the invasion and metastasis of tumor [25,26]. Thereby the assay was performed on both **APN** and **HDACs** so as to identify the selectivity of our target compounds, all the inhibition results are summarized in Tables 1 and 2. Bestatin was used as the positive control for **APN** inhibitor, while, SAHA was used as the positive control for **HDACs** inhibitor.

As shown in Tables 1 and 2, it is worthy to note that these ureido derivatives displayed dramatic selectivity towards **APN** over **HDACs**. These results, to a certain extent, validated our strategy for design of potential APNIs. As the above mentioned selectivity against APN, the following SARs were mainly discussed about APN inhibition.

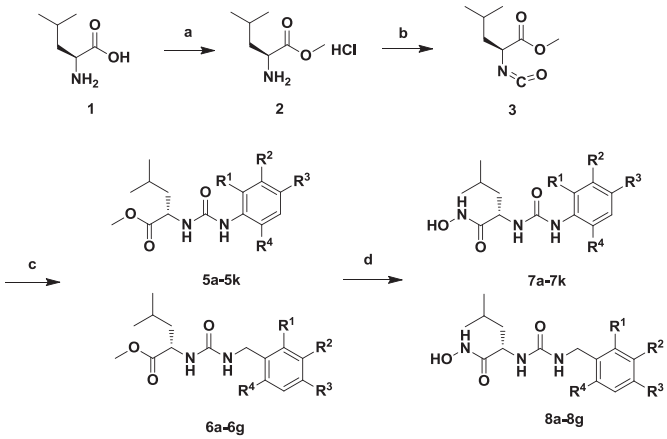

Scheme 1. Reagents and conditions: (a) acetyl chloride, MeOH, reflux; (b) triphosgene, $NaHCO_3$, DCM, ice-bath; (c) corresponding disubstituted anilines or benzylamines, DCM, room temperature; (d) NH_2OK, MeOH, 1 h.

Table 1
Structures and IC_{50} of 7a–7k against APN and HDACs.

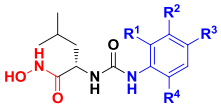

Compd	R^1	R^2	R^3	R^4	$IC_{50}(\mu M)$[a] APN	$IC_{50}(\mu M)$[a] HDAC
7a	Me	H	H	Me	0.02 ± 0.01	>100
7b	Et	H	H	Et	0.03 ± 0.02	>100
7c	iPr	H	H	iPr	0.05 ± 0.03	>100
7d	F	H	H	F	0.23 ± 0.14	>100
7e	Me	H	Me	Me	0.08 ± 0.02	>100
7f	Me	H	Me	H	0.18 ± 0.13	>100
7g	F	H	F	H	0.34 ± 0.19	>100
7h	Cl	H	Cl	H	0.56 ± 0.23	>100
7i	OMe	H	OMe	H	0.46 ± 0.23	>100
7j	H	F	OMe	H	0.42 ± 0.12	>100
7k	H	Cl	Me	H	0.09 ± 0.05	>100
4k	H	H	H	H	1.15 ± 0.53	>100
Bestatin	–	–	–	–	3.40 ± 0.03	>100
SAHA	–	–	–	–	–	0.12 ± 0.03

[a] Mean values and standard deviations of triplicate experiments are given.

Table 2
Structures and IC_{50} of 8a–8g against APN and HDACs.

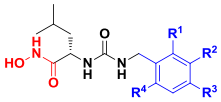

Compd	R^1	R^2	R^3	R^4	$IC_{50}(\mu M)$[a] APN	$IC_{50}(\mu M)$[a] HDAC
8a	F	H	H	F	0.69 ± 0.25	>100
8b	Cl	H	H	Cl	0.58 ± 0.14	>100
8c	F	H	F	H	0.33 ± 0.21	>100
8d	OMe	H	OMe	H	0.46 ± 0.19	>100
8e	H	F	F	H	0.42 ± 0.17	>100
8f	H	Me	Me	H	0.44 ± 0.16	>100
8g	Me	Me	H	H	0.07 ± 0.02	>100
4k	–	–	–	–	1.15 ± 0.53	>100
Bestatin	–	–	–	–	3.40 ± 0.03	>100
SAHA	–	–	–	–	–	0.12 ± 0.03

[a] Mean values and standard deviations of triplicate experiments are given.

Bioassay results indicate that all compounds exhibited better inhibitory activity against **APN** than the leading compound **4k**, some of which had 10-fold or more improvement. It may be due to the disubstitued groups on the phenyl group can enhance the interaction with the hydrophobic region of the enzyme. The activity of analogues with disubstituted anilines (**7a**–**7k**) is better than analogues with disubstituted benzylamines (**8a**–**8g**). Comparing **7a**–**7d** and **7f**–**7k**, we could find that the compounds containing ortho disubstituted phenyl groups have better activities than those containing other disubstituted phenyl groups. Among compounds **7a**–**7d** with ortho disubstitution, **7a**–**7c** with dialkyl groups on the benzene ring were more potent than **7d** with dihalogens. And different alkyl groups in aromatic ring also have different levels of impacts on their activities. The data shown in Table 1 suggested that the preferred substitutions against APN were, in decreasing order, methyl-substitution (**7a**) and ethyl-substitution (**7b**), followed by the isopropyl inhibitor (**7c**). It seems that methyl is the most favorable group for APN and bigger bulks lead to impaired activity. Compound with tri-substitution (**7e**) on the aromatic ring

was less potent than **7a**, which indicated that para-substitution was detrimental to APN inhibition.

Furthermore, we assessed the ability of compounds **7a**, **7b** for enzymatic inhibition on human APN derived from cultured ES-2 human ovarian carcinoma cells because of high APN expression. The results showed that both compounds **7a** ($IC_{50} = 0.12 \pm 0.05$ μM) and **7b** ($IC_{50} = 0.28 \pm 0.11$ μM) were still better than Bestatin (20.12 ± 1.26 μM), which was consistent with the above trends of our cell-free enzyme inhibitory activity.

The anti-invasion activities of **7a** and **7b** were evaluated by transwell chambers coated with Matrigel. According to the result, ES-2 cells could freely invade and pass through Matrigel in control group, while the invasion was significantly obstructed by bestatin, **7a** and **7b**. Consistent with the result of enzyme inhibitory activity, **7a** and **7b** were more potent than bestatin at the same concentration of 150 μM (Fig. 2), which indicated their potential therapeutic application in overcoming cancer metastasis.

To further examine its *in vivo* antimetastasis effect, compound **7a** was evaluated in the mouse hepatoma-22 (H22) pulmonary metastasis model. In this test, the numbers of marcroscopic metastatic nodes in the lungs were counted to evaluate the antimetastasis effects of tested compounds. As shown in Fig. 3, the inhibitory rate of compound **7a** (91.7%) at the dosage of 80 mg/kg is higher than that of Bestatin (75.9%), which indicates that compound **7a** with promising potential in application for antimetastasis therapy deserves further research and development in the pre-clinical studies.

4. Conclusion

In all, one series of novel potent leucine ureido derivative as APN inhibitors have been synthesized and evaluated. The preliminary results showed that most of the target compounds exhibit better inhibition than the positive control Bestatin and our lead compound **4k**. These results suggest that introduction of disubstitution on ortho-position of phenyl group of **4k** could result in analogs with improved APN inhibitory activities, such as **7a** which could be used as new lead for further structure optimization in the future APNIs exploration.

5. Experiment

5.1. Chemistry: general procedures

All the materials involved were purchased from commercial suppliers. Solvents were distilled prior to use. All the reactions were

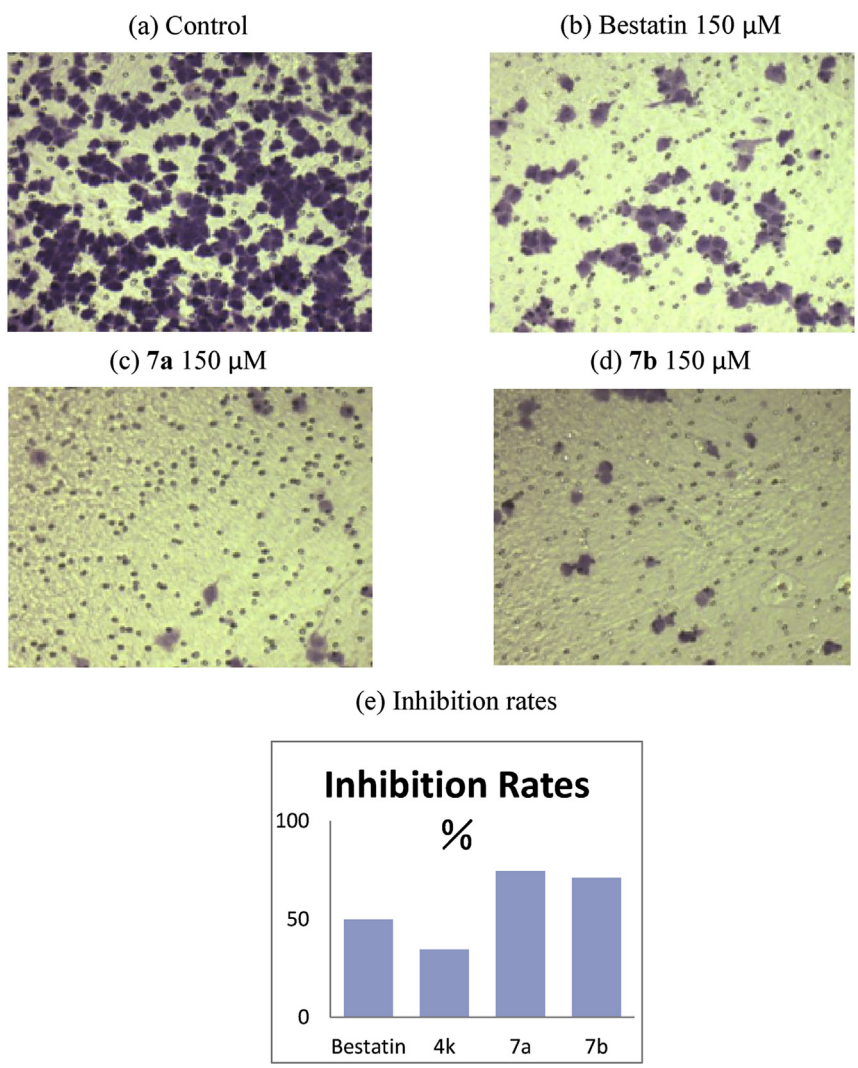

Fig. 2. ES-2 cell invasion inhibition: (a) control; (b) Bestatin, 150 μM; (c) **7a,** 150 μM; (d) **7b,** 150 μM; (e) The inhibitory rates of compounds **4k**, **7a**, **7b** and Bestatin against ES-2 cell invasion under the concentration of 150 μM. Data expressed are mean values of three independent experiments.

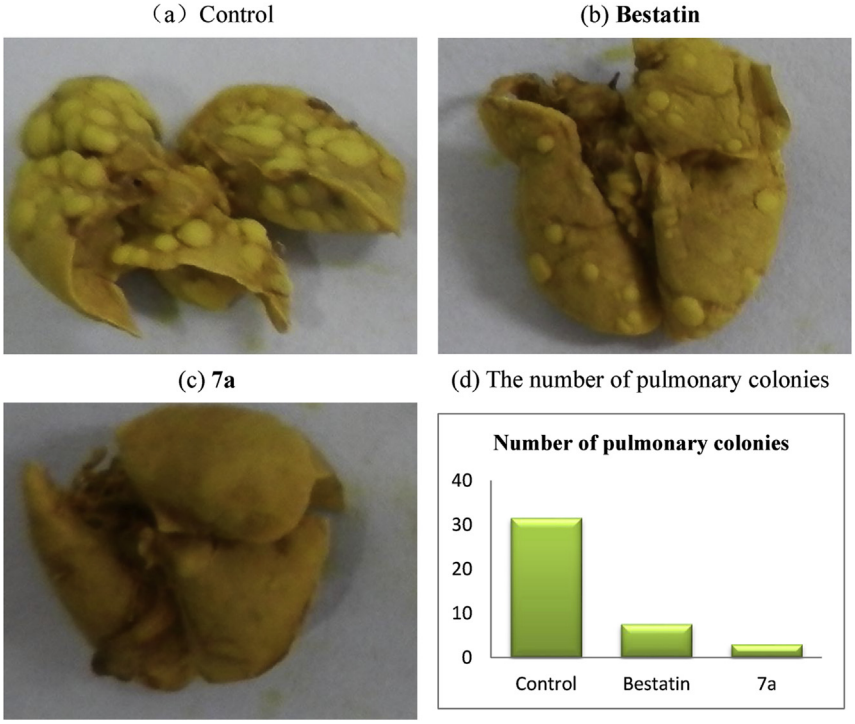

Fig. 3. The result of *in vivo* H22 cell metastasis assay.

monitored by thin-layer chromatography on 0.25 mm silica gel plates (60 GF-254) and visualized with UV light or chloride ferric. The products were purified by column chromatography which was performed using 200–300 mesh silica gel. NMR spectra were determined on a Brucker Avance 600 spectrometer, δ in parts per million and *J* in Hertz. TMS was used as an internal standard. ESI-MS were determined on an API 4000 spectrometer. Measurements were made in DMSO-*d6* solutions. Melting points were tested using an electrothermal melting point apparatus and were uncorrected.

5.2. General procedure for the synthesis of **7a**–**7k** and **8a**–**8g**

To a mixture of L-leucine methyl ester hydrochloride (1.8 g, 10 mmol) in saturated $NaHCO_3$ (36 mL) and DCM (36 mL) was added triphosgene (0.98 g, 3.3 mmol). The reaction mixture was vigorously stirred under ice-water bath for 1 h and the organic layer was collected. The water layer was extracted with DCM for three times and the organic phases were combined and dried with $MgSO_4$. After the solvent removed under vacuum, the residue was dissolved in DCM (20 mL). This solution was then added to corresponding disubstituted anilines or benzylamines (10 mmol) in DCM (40 mL) under ice bath. The reaction mixture was stirred at room temperature for 12 h and then the solvent was removed under reduce pressure. The residue was taken up with ethyl acetate (100 mL) and washed with 1 N HCl (30 mL) and brine (30 mL). The organic phase was dried with $MgSO_4$. After the solvent removed, the residue without purification was directly added to a solution of potassium hydroxylamine (4.18 g, 28 mmol) in methanol (10 mL). The reaction mixture was stirred at room temperature for 1 h and then removed methanol under reduce pressure. The residue was taken up with 1 N HCl and extracted with ethyl acetate. The organic phase was washed with brine and dried with $MgSO_4$. After the solvent removed under reduce pressure, the residue was separated by silica gel column chromatography to afford **7a**–**7k** and **8a**–**8g**, respectively.

5.2.1. (S)-2-[3-(2,6-Dimethyl-phenyl)-ureido]-4-methyl-pentanoic acid hydroxyamide (**7a**)

White powder, yield 49%, mp = 173–175 °C; ^{1}HNMR (600 MHz, DMSO-d_6): δ10.72 (s, 1H), 8.85 (s, 1H), 7.57 (s, 1H), 7.05–6.98 (m, 3H), 6.25 (s, 1H), 4.17–4.13 (m, 1H), 2.13 (s, 6H), 1.64–1.57 (m, 1H), 1.44–1.35 (m, 2H), 0.90 (d, 3H, J = 6.6 Hz), 0.88 (d, 3H, J = 6.6 Hz), ^{13}C-NMR (150 MHz, DMSO-*d6*): δ 169.2, 155.0, 135.7, 135.2, 127.5, 125.4, 48.9, 42.6, 24.1, 22.7, 22.0, 18.0; HRMS (AP-ESI): m/*z*: Calcd for $[C_{15}H_{23}N_3O_3+H]^+$: 294.1812; Found: 294.1816 $[M+H]^+$.

5.2.2. (S)-2-[3-(2,6-Diethyl-phenyl)-ureido]-4-methyl-pentanoic acid hydroxyamide (**7b**)

White powder, yield 40%, mp = 179–180 °C; ^{1}HNMR (600 MHz, DMSO-d_6): δ10.73 (s, 1H), 8.87 (s, 1H), 7.51 (s, 1H), 7.11–7.01 (m, 3H), 6.49–6.25 (m, 1H), 4.18–4.12 (m, 1H), 2.50 (q, 4H, J = 7.8 Hz), 1.65–1.57 (m, 1H), 1.44–1.33 (m, 2H), 1.08 (t, 6H, J = 7.8 Hz), 0.90 (d, 3H, J = 6.6 Hz), 0.88 (d, 3H, J = 6.6 Hz); ^{13}C-NMR (150 MHz, DMSO-*d6*): δ 169.3, 155.6, 141.7, 134.4, 126.2, 125.8, 48.8, 42.8, 24.3, 24.1, 22.7, 21.9, 14.5; HRMS (AP-ESI): m/*z*: Calcd for $[C_{17}H_{27}N_3O_3+H]^+$: 322.2125; Found: 322.2122 $[M+H]^+$.

5.2.3. (S)-2-[3-(2,6-Diisopropyl-phenyl)-ureido]-4-methyl-pentanoic acid hydroxyamide (**7c**)

White powder, yield 48%, mp = 177–178 °C; ^{1}HNMR (600 MHz, DMSO-d_6): δ10.77 (s, 1H), 8.90 (s, 1H), 7.49 (s, 1H), 7.24–7.18 (m, 1H), 7.14–7.12 (m, 2H), 6.41–6.39 (m, 1H), 4.22–4.19 (m, 1H), 3.14–3.12 (m, 2H), 1.66–1.64 (m, 1H), 1.48–1.44 (m, 2H), 1.14 (d, 6H, J = 6.0 Hz), 1.12 (d, 6H, J = 6.0 Hz), 0.93 (d, 3H, J = 6.0 Hz), 0.90 (d, 3H, J = 6.0 Hz); ^{13}C-NMR (150 MHz, DMSO-*d6*): δ 169.6, 155.7, 146.9, 133.4, 127.3, 123.1, 48.7, 41.2, 24.6, 24.1, 22.8, 21.9, 14.5; HRMS (AP-ESI): m/*z*: Calcd for $[C_{19}H_{31}N_3O_3 +H]^+$: 350.2438; Found: 350.2441 $[M+H]^+$.

*5.2.4. (S)-2-[3-(2,6-Difluoro-phenyl)-ureido]-4-methyl-pentanoic acid hydroxyamide (**7d**)*

White powder, yield 61%, mp = 163–165 °C; ^{1}HNMR (600 MHz, DMSO-d_6): δ10.78 (s, 1H), 8.90 (s, 1H), 7.93 (s, 1H), 7.28–7.18 (m, 1H), 7.10 (d, 1H, J = 7.8 Hz), 7.08 (d, 1H, J = 7.8 Hz), 6.57 (d, 1H, J = 9.0 Hz), 4.18–4.06 (m, 1H), 1.61–1.51 (m, 1H), 1.44–1.36 (m, 2H), 0.90 (d, 3H, J = 6.6 Hz), 0.88 (d, 3H, J = 6.6 Hz); ^{13}C-NMR (150 MHz, DMSO-*d6*): δ 169.3, 159.0, 157.3, 154.7, 126.7, 116.2, 112.1, 112.0, 49.6, 43.0, 24.7, 23.1, 22.6; HRMS (AP-ESI): m/*z*: Calcd for $[C_{13}H_{17}F_2N_3O_3+H]^+$ 302.1311; Found: 302.1312 $[M+H]^+$.

*5.2.5. (S)-2-[3-(2,4,6-Trimethyl-phenyl)-ureido]-4-methyl-pentanoic acid hydroxyamide (**7e**)*

White powder, yield 40%, mp = 183–175 °C; ^{1}HNMR (600 MHz, DMSO-d_6): δ10.72 (s, 1H), 8.86 (s, 1H), 7.45 (s, 1H), 6.83 (s, 2H), 6.21 (m, 1H), 4.18–4.10 (m, 1H), 2.20 (s, 3H), 2.08 (s, 6H), 1.63–1.54 (m, 1H), 1.44–1.31 (m, 2H), 0.89 (d, 3H, J = 6.6 Hz), 0.87 (d, 3H, J = 6.6 Hz); ^{13}C-NMR (150 MHz, DMSO-*d6*): δ 169.2, 155.2, 135.1, 134.4, 133.0, 128.1, 48.9, 42.6, 24.1, 22.7, 22.0, 20.3, 17.9; HRMS (AP-ESI): m/*z*: Calcd for $[C_{16}H_{25}N_3O_3+H]^+$ 308.1969; Found: 308.1970 $[M+H]^+$.

*5.2.6. (S)-2-[3-(2,4-Dimethyl-phenyl)-ureido]-4-methyl-pentanoic acid hydroxyamide (**7f**)*

White powder, yield 53%, mp = 163–164 °C; ^{1}HNMR (600 MHz, DMSO-d_6): δ10.78 (s, 1H), 8.86 (s, 1H), 7.67 (s, 1H), 7.66 (d, 1H, J = 7.2 Hz), 6.92 (s, 1H), 6.88 (d, 1H, J = 7.2 Hz), 6.74 (d, 1H, J = 9.0 Hz), 4.17–4.11 (m, 1H), 2.19 (s, 3H), 2.13 (s, 3H), 1.62–1.53 (m, 1H), 1.42–1.38 (m, 2H), 0.91 (d, 3H, J = 6.6 Hz), 0.88 (d, 3H, J = 6.6 Hz); ^{13}C-NMR (150 MHz, DMSO-*d6*): δ 168.9, 154.5, 135.2, 130.4, 126.4, 126.3, 120.2, 48.8, 42.3, 24.1, 22.6, 22.0, 20.1, 17.6; HRMS (AP-ESI): m/*z*: Calcd for $[C_{15}H_{23}N_3O_3+H]^+$ 294.1812; Found: 294.1811$[M+H]^+$.

*5.2.7. (S)-2-[3-(2,4-Difluoro-phenyl)-ureido]-4-methyl-pentanoic acid hydroxyamide (**7g**)*

White powder, yield 70%, mp = 165–166 °C; ^{1}HNMR (600 MHz, DMSO-d_6): δ10.79 (s, 1H), 8.87 (s, 1H), 8.38 (s, 1H), 8.07–8.05 (m, 1H),7.25–7.23 (m, 1H), 6.98 (m, 1H), 6.87 (d, 1H, J = 8.4 Hz), 4.15–4.12 (m, 1H), 1.58–1.56 (m, 1H), 1.44–1.33 (m, 2H), 0.91 (d, 3H, J = 6.6 Hz), 0.88 (d, 3H, J = 6.6 Hz); ^{13}C-NMR (150 MHz, DMSO-*d6*): δ 169.3, 156.7, 154.7, 151.8, 125.2, 121.4, 111.3, 104.0, 49.4, 42.7, 24.7, 23.1, 22.5; HRMS (AP-ESI): m/*z*: Calcd for $[C_{13}H_{17}F_2N_3O_3+H]^+$ 302.1311; Found: 302.1312 $[M+H]^+$.

*5.2.8. (S)-2-[3-(2,4-Dichloro-phenyl)-ureido]-4-methyl-pentanoic acid hydroxyamide (**7h**)*

White powder, yield 45%, mp = 165–167 °C; ^{1}HNMR (600 MHz, DMSO-d_6): δ10.77 (s, 1H), 8.85 (s, 1H), 8.23 (s, 1H), 8.16 (d, 1H, J = 8.4 Hz), 7.52 (s, 1H), 7.37 (d, 1H, J = 8.4 Hz), 7.28 (d, 1H, J = 8.4 Hz), 4.13–4.12 (m, 1H), 1.56–1.51 (m, 1H), 1.40–1.37 (m, 2H), 0.88 (d, 3H, J = 6.6 Hz), 0.85 (d, 3H, J = 6.6 Hz); ^{13}C-NMR (150 MHz, DMSO-*d6*): δ 169.2, 154.4, 136.3, 128.9, 127.9, 125.5, 122.0, 121.7, 49.5, 42.6, 24.7, 23.1, 22.5; HRMS (AP-ESI): m/*z*: Calcd for $[C_{13}H_{17}Cl_2N_3O_3+H]^+$ 334.0722; Found: 334.0724 $[M+H]^+$.

*5.2.9. (S)-2-[3-(2,4-Dimethoxy-phenyl)-ureido]-4-methyl-pentanoic acid hydroxyamide (**7i**)*

White powder, yield 82%, mp = 178–180 °C; ^{1}HNMR (600 MHz, DMSO-d_6): δ10.73 (s, 1H), 8.81 (s, 1H), 7.87–7.84 (m, 2H), 6.95 (d, 1H, J = 8.4 Hz), 6.55 (d, 1H, J = 1.8 Hz), 6.41 (dd, 1H, J = 8.4, 1.8 Hz), 4.11–4.09 (m, 1H), 3.80 (s, 3H), 3.70 (s, 3H), 1.60–1.52 (m, 1H), 1.44–1.33 (m, 2H), 0.90 (d, 3H, J = 6.6 Hz), 0.87 (d, 3H, J = 6.6 Hz); ^{13}C-NMR (150 MHz, DMSO-*d6*): δ 169.7, 155.2, 154.7, 149.1, 123.1, 119.5, 104.4, 99.1, 56.1, 55.6, 49.4, 42.6, 24.7, 23.2, 22.5; HRMS (AP-ESI): m/*z*: Calcd for $[C_{15}H_{23}N_3O_5+H]^+$ 326.1710; Found: 326.1713 $[M+H]^+$.

*5.2.10. (S)-2-[3-(3-Fluoro-4-methoxy-phenyl)-ureido]-4-methyl-pentanoic acid hydroxyamide (**7j**)*

White powder, yield 49%, mp = 159–161 °C; ^{1}HNMR (600 MHz, DMSO-d_6): δ10.80 (s, 1H), 8.90 (s, 1H), 8.57 (s, 1H), 7.45 (d, 1H, J = 14.4 Hz), 7.05 (t, 1H, J = 9.0 Hz), 6.95 (d, 1H, J = 8.4 Hz), 6.32 (d, 1H, J = 9.0 Hz), 4.17–4.12 (m, 1H), 3.79 (s, 3H), 1.62–1.58 (m, 1H), 1.44–1.33 (m, 2H), 0.93 (d, 3H, J = 6.6 Hz), 0.90 (d, 3H, J = 6.6 Hz); ^{13}C-NMR (150 MHz, DMSO-*d6*): δ 174.2, 159.7, 156.3, 146.5, 139.2, 119.6, 118.3, 110.0, 61.4, 54.1, 47.6, 29.4, 27.9, 27.3; HRMS (AP-ESI): m/*z*: Calcd for $[C_{14}H_{20}FN_3O_4 +H]^+$ 314.1511; Found: 314.1513 $[M+H]^+$.

*5.2.11. (S)-2-[3-(3-Chloro-4-Methyl-phenyl)-ureido]-4-methyl-pentanoic acid hydroxyamide (**7k**)*

White powder, yield 68%, mp = 156–158 °C; ^{1}HNMR (600 MHz, DMSO-d_6): δ10.82 (s, 1H), 8.91 (s, 1H), 8.66 (s, 1H), 7.65 (s, 1H), 7.20 (d, 1H, J = 7.8 Hz), 7.07 (d, 1H, J = 8.4 Hz), 6.39 (d, 1H, J = 9.0 Hz), 4.16–4.13 (m, 1H), 2.25 (s, 3H), 1.62–1.57 (m, 1H), 1.44–1.40 (m, 2H), 0.93 (d, 3H, J = 6.6 Hz), 0.91 (d, 3H, J = 6.6 Hz); ^{13}C-NMR (150 MHz, DMSO-*d6*): δ 169.4, 154.8, 139.9, 133.5, 131.5, 127.9, 117.8, 116.6, 49.3, 42.8, 24.7, 23.2, 22.6, 19.2; HRMS (AP-ESI): m/*z*: Calcd for $[C_{14}H_{20}ClN_3O_3+H]^+$ 314.1266; Found: 314.1264 $[M+H]^+$.

*5.2.12. (S)-2-[3-(2,6-Difluoro-benzyl)-ureido]-4-methyl-pentanoic acid hydroxyamide (**8a**)*

White powder, yield 47%, mp = 161–163 °C; ^{1}HNMR (600 MHz, DMSO-d_6): δ10.70 (s, 1H), 8.81 (s, 1H), 7.41–7.38 (m, 1H), 7.10 (t, 2H, J = 7.8 Hz), 6.40–6.38 (m, 1H), 6.10 (d, 1H, J = 9.0 Hz), 4.37–4.23 (m, 2H), 4.08–4.04 (m, 1H), 1.54–1.50 (m, 1H), 1.37–1.28 (m, 2H), 0.89 (d, 3H, J = 6.6 Hz), 0.86 (d, 3H, J = 6.6 Hz); ^{13}C-NMR (150 MHz, DMSO-*d6*): δ 169.7, 157.2, 130.1, 112.0, 111.9, 110.0, 49.4, 42.9, 31.4, 24.6, 23.1, 22.6; HRMS (AP-ESI): m/*z*: Calcd for $[C_{14}H_{19}F_2N_3O_3+H]^+$ 316.1467; Found: 316.1472 $[M+H]^+$.

*5.2.13. (S)-2-[3-(2,6-Dichloro-benzyl)-ureido]-4-methyl-pentanoic acid hydroxyamide (**8b**)*

White powder, yield 48%, mp = 175–176 °C; ^{1}HNMR (600 MHz, DMSO-d_6): δ10.70 (s, 1H), 8.81 (s, 1H), 7.48 (d, 2H, J = 7.8 Hz), 7.34 (t, 1H, J = 7.8 Hz), 6.26 (t, 1H, J = 4.8 Hz), 6.11 (d, 1H, J = 9.0 Hz), 4.50–4.40 (m, 2H), 4.09–4.03 (m, 1H), 1.53–1.48 (m, 1H), 1.37–1.28 (m, 2H), 0.87 (d, 3H, J = 6.6 Hz), 0.85 (d, 3H, J = 6.6 Hz); ^{13}C-NMR (150 MHz, DMSO-*d6*): δ 169.1, 156.6, 135.1, 134.5, 129.9, 128.5, 48.9, 42.3, 39.9, 24.0, 22.5, 22.1; HRMS (AP-ESI): m/*z*: Calcd for $[C_{14}H_{19}Cl_2N_3O_3+H]^+$ 348.0876; Found:348.0876 $[M+H]^+$.

*5.2.14. (S)-2-[3-(2,4-Difluoro-benzyl)-ureido]-4-methyl-pentanoic acid hydroxyamide (**8c**)*

White powder, yield 60%, mp = 172–173 °C; ^{1}HNMR (600 MHz, DMSO-d_6): δ10.70 (s, 1H), 8.83 (s, 1H), 7.37–7.32 (m, 1H), 7.25–7.20 (m, 1H), 7.10–7.06 (m, 1H), 6.46 (t, 1H, J = 6.0 Hz), 6.20 (d, 1H, J = 8.4 Hz), 4.23–4.21 (m, 2H), 4.10–4.09 (m, 1H), 1.57–1.52 (m, 1H), 1.40–1.33 (m, 2H), 0.90 (d, 3H, J = 6.0 Hz), 0.87 (d, 3H, J = 6.0 Hz); ^{13}C-NMR (150 MHz, DMSO-*d6*): δ 169.2, 161.1, 159.7, 157.0, 130.2, 123.6, 111.0, 103.4, 48.9, 42.3, 36.1, 24.2, 22.6, 22.0; HRMS (AP-ESI): m/*z*: Calcd for $[C_{14}H_{19}F_2N_3O_3+H]^+$ 316.1467; Found: 316.1470 $[M+H]^+$.

*5.2.15. (S)-2-[3-(2,4-Dimethoxy-benzyl)-ureido]-4-methyl-pentanoic acid hydroxyamide (**8d**)*

White powder, yield 66%, mp = 175–177 °C; ^{1}HNMR (600 MHz, DMSO-d_6): δ10.66 (s, 1H), 8.78 (s, 1H), 7.04 (d, 1H, J = 7.8 Hz), 6.53 (s, 1H), 6.45 (d, 1H, J = 8.4 Hz), 6.16 (t, 1H, J = 6.0 Hz), 6.13 (d, 1H,

J = 9.6 Hz), 4.08–4.02 (m, 3H), 3.78 (s, 3H), 3.73 (s, 3H), 1.55–1.50 (m, 1H), 1.34–1.30 (m, 2H), 0.87 (d, 3H, J = 6.6 Hz), 0.85 (d, 3H, J = 6.6 Hz); ^{13}C-NMR (150 MHz, DMSO-*d6*): **δ** 169.4, 159.4, 157.5, 157.1, 128.6, 120.1, 104.0, 98.0, 55.2, 55.0, 48.8, 42.3, 37.7, 24.0, 22.6, 22.0; HRMS (AP-ESI): m/*z*: Calcd for $[C_{16}H_{25}N_3O_5 + H]^+$ 340.1794; Found: 340.1768$[M+H]^+$.

5.2.16. (S)-2-[3-(3,4-Difluoro-benzyl)-ureido]-4-methyl-pentanoic acid hydroxyamide (***8e***)

White powder, yield 61%, mp = 173–174 °C; ^{1}HNMR (600 MHz, DMSO-d_6): **δ**10.67 (s, 1H), 8.80 (s, 1H), 7.40–7.34 (m, 1H), 7.26–7.22 (m, 1H), 7.07 (s, 1H), 6.48 (t, 1H, J = 6.6 Hz), 6.20 (d, 1H, J = 9.0 Hz), 4.20–4.18 (m, 2H), 4.10–4.05 (m, 1H), 1.56–1.51 (m, 1H), 1.37–1.33 (m, 2H), 0.88 (d, 3H, J = 6.6 Hz), 0.85 (d, 3H, J = 6.6 Hz); ^{13}C-NMR (150 MHz, DMSO-*d6*): **δ** 169.8, 157.8, 149.9, 148.4, 139.3, 124.0, 117.7, 116.2, 49.6, 42.9, 42.6, 24.6, 23.2, 22.6; HRMS (AP-ESI): m/*z*: Calcd for $[C_{14}H_{19}F_2N_3O_3 + H]^+$ 316.1467; Found: 316.1471$[M+H]^+$.

5.2.17. (S)-2-(3-(3,4-Dimethylbenzyl)ureido)-N-hydroxy-4-methylpentanamide (***8f***)

White powder, yield 57%, mp = 170–171 °C; ^{1}HNMR (600 MHz, DMSO-d_6): **δ**10.68 (s, 1H), 8.80 (s, 1H), 7.05 (d, 1H, J = 7.8 Hz), 6.98 (s, 1H), 6.93 (d, 1H, J = 7.8 Hz), 6.32 (t, 1H, J = 6.0 Hz), 6.09 (d, 1H, J = 9.0 Hz), 4.12–4.06 (m, 3H), 2.18 (s, 3H), 2.17 (s, 3H), 1.57–1.51 (m, 1H), 1.34 (t, 2H, J = 7.2 Hz), 0.88 (d, 3H, J = 6.6 Hz), 0.86 (d, 3H, J = 6.6 Hz); ^{13}C-NMR (150 MHz, DMSO-*d6*): **δ** 169.3, 157.2, 137.7, 135.7, 134.1, 129.1, 128.1, 124.3, 48.9, 42.4, 39.9, 24.1, 22.6, 22.0, 19.2, 18.8; HRMS (AP-ESI): m/*z*: Calcd for $[C_{16}H_{25}N_3O_3 + Na]^+$ 330.1788; Found: 330.1780$[M+Na]^+$.

5.2.18. (S)-2-[3-(2,3-Dimethyl-benzyl)-ureido]-4-methyl-pentanoic acid hydroxyamide (***8g***)

White powder, yield 51%, mp = 166–167 °C; ^{1}HNMR (600 MHz, DMSO-d_6): **δ**10.66 (s, 1H), 8.77 (s, 1H), 7.37 (t, 1H, J = 7.2 Hz), 7.08 (d, 1H, J = 7.2 Hz), 7.07 (d, 1H, J = 7.2 Hz), 7.07 (d, 1H, J = 7.2 Hz), 6.36 (t, 1H, J = 6.0 Hz), 6.06 (d, 1H, J = 9.0 Hz), 4.21–4.17 (m, 2H), 4.10–4.05 (m, 1H), 2.23 (s, 3H), 2.13 (s, 3H),1.56–1.51 (m, 1H), 1.35–1.30 (m, 2H), 0.88 (d, 3H, J = 6.6 Hz), 0.85 (d, 3H, J = 6.6 Hz); ^{13}C-NMR (150 MHz, DMSO-*d6*): **δ** 169.9, 157.8, 138.3, 136.2, 134.7, 129.7, 128.7, 124.8, 49.5, 43.0, 42.9, 24.7, 23.2, 22.6, 19.9, 19.4; HRMS (AP-ESI): m/*z*: Calcd for $[C_{16}H_{25}N_3O_3+H]^+$ 308.1969; Found: 308.1968 $[M+H]^+$.

5.3. Biological materials and methods

5.3.1. Materials

5.3.1.1. Chemicals. Chemicals was synthesized as mentioned above and dissolved in dimethylsulfoxide (DMSO) or PBS and diluted to the required concentration with culture medium when used.

5.3.1.2. Cell line and cell culture. The human leukemia cell line, ES-2 and HL-60 were obtained from the Institute of National Cancer Research of China (Beijing, China). Cells were maintained in RPMI-1640 supplemented with 10% (v/v) heat-inactivated fetal bovine serum, penicillin–streptomycin (100 IU/ml–100 mg/mL), 2 mM glutamine, and 10 mM Hepes buffer at 37 °C in a humid atmosphere (5% CO_2–95% air).

5.3.2. In vitro APN enzyme assay

IC_{50} values against APN were determined by using L-leu-p-nitroanilide as substrate and Microsomal aminopeptidase from Porcine Kidney Microsomes (Sigma) as enzyme in 50 mM PBS (PH 7.2) or suspension of ES-2 cells in PBS (1×10^5/well). After adding the detected compounds, the solution with various concentrations was incubated with APN at 37 °C for 5 min. Then the solution of substrate was added into the above mixture, which was incubated for another 30 min at 37 °C. The hydrolysis of the substrate was measured by following the change in the absorbance monitored at 405 nm with a plate reader (Varioskan, Thermo, USA).

5.3.3. In vitro HDACs inhibition assay

In vitro HDACs inhibitory activity assay was determined by using Boc-Lys (acetyl)-AMC as substrate and Hela nuclear extract (mainly containing HDAC1 and HDAC2) as enzymes in 15 mM Tris–HCl (PH 8.0) at 37 °C. First, 10 μL of enzymes solution was added to tested compounds solutions at various concentrations (50 μL) and incubated for 5 min at 37 °C. Then 40 μL of substrate was added and the mixture continued to incubate for another 30 min in the same environment. Finally, 100 μL of developer which containing trypsin and TSA was putted into the mixture. Twenty minutes later, fluorescence intensity was measured at 390 nm excitation and 460 nm emission wavelengths with a microplate reader.

5.3.4. Enzyme inhibitory assay towards APN from ES-2 cells

$\mathbf{IC_{50}}$ values against **APN** were determined by using L-Leu-p-nitroanilide as substrate and ES-2 human ovarian clear cell carcinoma cells as the enzyme source. In brief, the assay was performed in 96-well plates in 10 mM PBS, pH 7.4 as the assay buffer, at 37 °C. All solutions of inhibitors were prepared in the assay buffer with 0.2% DMSO in final concentration as the fluxing agent. Compounds were pre-incubated with ES-2 cell suspension (1×10^5 cells per well) for 5 min at room temperature. The assay mixture, which contained 20 μL of the inhibitor solution (concentration dependent on the inhibitors), 70 μL of the ES-2 cell suspension, 10 μL of the substrate solution, or the assay buffer, was adjusted to 100 μL, and then incubated at 37 °C for 1 h. The hydrolysis of the substrate in the supernatant liquor after centrifugation was monitored with the UV–Vis spectrophotometer Pharmacia LKB, Biochrom 4060. The enzyme activity inhibitory rate was calculated from the photometric intensity readings, and the $\mathbf{IC_{50}}$ was determined through a regression analysis of the concentration/inhibitory rate data.

5.3.5. Anti-invasion assay

The BD BioCoat™ Matrigel™ Invasion Chambers were rehydrated with 500 μL RPMI-1640 culture medium with 1% FBS in both of the upper and lower chambers for 2 h. After the medium was removed, 750 μL of RPMI-1640 culture medium with 10% FBS were added to the lower chambers. Target compounds in 100 μL of RPMI-1640 culture medium with 1% FBS were added to the upper chamber at the same time. Cells in 400 μL of RPMI-1640 culture medium with 1% FBS (1×10^5 cells per well) were added and allowed to invade for 8 h at 37 °C in a CO_2 incubator. 8 h later, Matrigel and cells in the upper chamber were removed with a cotton swab. The remaining cells were fixed, stained with 0.1% crystal violet, and photographs were taken under a microscope. **ES-2** invasion was quantified by counting the number of cells in five random fields (×100) per insert.

5.3.6. Anti-metastasis assay in vivo

Mice bearing H22 tumor were injected via the caudal vein and randomly divided into 3 groups. The animals of the control group were treated with the same volume of excipient, while the other groups were given the inhibitors (**7a** and bestatin) by oral administration, at a dose of 80 mg/kg/day, 6 days/week for 2 weeks. The mice were then weighed and sacrificed for autopsy immediately. The lungs with tumor nodes were removed, weighed, and then placed in bouin stationary solution (saturated 2,4,6-trinitrophenol solution/formaldehyde/glacial acetic acid = 15:5:1). One day later, the metastasized nodes on the surface of lungs were counted.

Acknowledgments

This work was supported by National High-Tech R&D Program of China (863 Program) (Grant No. 2014AA020523), National Natural Science Foundation of China (Grant Nos. 21302111, 81373282, 21172134).

Appendix A. Supplementary data

Supplementary data related to this article can be found at http://dx.doi.org/10.1016/j.ejmech.2015.11.021.

References

[1] R.A. Ashmun, A.T. Look, Metalloprotease activity of CD13/aminopeptidase N on the surface of human myeloid cells, Blood 75 (1990) 462–469.
[2] A.A. Amoscato, R.M. Sramkoski, G.F. Babcock, J.W. Alexander, Neutral surface aminopeptidase activity of human tumor cell lines, Biochim. Biophys. Acta (BBA) Protein Struct. Mol. Enzym. 1041 (1990) 317–319.
[3] L. Guzman-Rojas, R. Rangel, A. Salameh, J.K. Edwards, E. Dondossola, Y.-G. Kim, A. Saghatelian, R.J. Giordano, M.G. Kolonin, F.I. Staquicini, Cooperative effects of aminopeptidase N (CD13) expressed by nonmalignant and cancer cells within the tumor microenvironment, Proc. Natl. Acad. Sci. 109 (2012) 1637–1642.
[4] C. Antczak, I. De Meester, B. Bauvois, Transmembrane proteases as disease markers and targets for therapy, J. Biol. Regul. Homeost. Agents 15 (2000) 130–139.
[5] R. Pasqualini, E. Koivunen, R. Kain, J. Lahdenranta, M. Sakamoto, A. Stryhn, R.A. Ashmun, L.H. Shapiro, W. Arap, E. Ruoslahti, Aminopeptidase N is a receptor for tumor-homing peptides and a target for inhibiting angiogenesis, Cancer Res. 60 (2000) 722–727.
[6] N. Haraguchi, H. Ishii, K. Mimori, F. Tanaka, M. Ohkuma, H.M. Kim, H. Akita, D. Takiuchi, H. Hatano, H. Nagano, CD13 is a therapeutic target in human liver cancer stem cells, J. Clin. Investig. 120 (2010) 3326.
[7] I. Martin-Padura, P. Marighetti, A. Agliano, F. Colombo, L. Larzabal, M. Redrado, A.-M. Bleau, C. Prior, F. Bertolini, A. Calvo, Residual dormant cancer stem-cell foci are responsible for tumor relapse after antiangiogenic metronomic therapy in hepatocellular carcinoma xenografts, Lab. Investig. 92 (2012) 952–966.
[8] H. Nagano, H. Ishii, S. Marubashi, N. Haraguchi, H. Eguchi, Y. Doki, M. Mori, Novel therapeutic target for cancer stem cells in hepatocellular carcinoma, J. Hepato Biliary Pancreat. Sci. 19 (2012) 600–605.
[9] H. Suda, T. Takita, T. Aoyagi, H. Umezawa, The structure of bestatin, J. Antibiot. 29 (1976) 100–101.
[10] S. Yoshida, Y. Nakamura, H. Naganawa, T. Aoyagi, T. Takeuchi, Probestin, a new inhibitor of aminopeptidase M, produced by Streptomyces azureus MH663-2F6. II. Structure determination of probestin, J. Antibiot. 43 (1990) 149–153.
[11] M.-C. Chung, H.-J. Lee, H.-K. Chun, C.-H. Lee, S.-I. Kim, Y.-H. Kho, Bestatin analogue from Streptomyces neyagawaensis SL-387, Biosci. Biotechnol. Biochem. 60 (1996) 898–900.
[12] B.R. Lampret, J. Kidrič, B. Kralj, L. Vitale, M. Pokorny, M. Renko, Lapstatin, a new aminopeptidase inhibitor produced by Streptomyces rimosus, inhibits autogenous aminopeptidases, Arch. Microbiol. 171 (1999) 397–404.
[13] D.H. Rich, B.J. Moon, S. Harbeson, Inhibition of aminopeptidases by amastatin and bestatin derivatives. Effect of inhibitor structure on slow-binding processes, J. Med. Chem. 27 (1984) 417–422.
[14] L. Andersson, T.C. Isley, R. Wolfenden, alpha-Aminoaldehydes: transition state analog inhibitors of leucine aminopeptidase, Biochemistry 21 (1982) 4177–4180.
[15] R. Grzywa, J. Oleksyszyn, First synthesis of α-aminoalkyl-(N-substituted) thiocarbamoyl-phosphinates: inhibitors of aminopeptidase N (APN/CD13) with the new zinc-binding group, Bioorg. Med. Chem. Lett. 18 (2008) 3734–3736.
[16] A.B. Shenvi, alpha.-Aminoboronic acid derivatives: effective inhibitors of aminopeptidases, Biochemistry 25 (1986) 1286–1291.
[17] Q. Wang, M. Chen, H. Zhu, J. Zhang, H. Fang, B. Wang, W. Xu, Design, synthesis, and QSAR studies of novel lysine derives as amino-peptidase N/CD13 inhibitors, Bioorg. Med. Chem. 16 (2008) 5473–5481.
[18] J. Mou, H. Fang, F. Jing, Q. Wang, Y. Liu, H. Zhu, L. Shang, X. Wang, W. Xu, Design, synthesis and primary activity evaluation of L-arginine derivatives as amino-peptidase N/CD13 inhibitors, Bioorg. Med. Chem. 17 (2009) 4666–4673.
[19] Q. Li, H. Fang, X. Wang, L. Hu, W. Xu, Novel cyclic-imide peptidomimetics as aminopeptidase N inhibitors. Design, chemistry and activity evaluation. Part I, Eur. J. Med. Chem. 44 (2009) 4819–4825.
[20] Q. Li, H. Fang, X. Wang, W. Xu, Novel cyclic-imide peptidomimetics as aminopeptidase N inhibitors. Structure-based design, chemistry and activity evaluation. II, Eur. J. Med. Chem. 45 (2010) 1618–1626.
[21] C. Ma, X. Li, K. Jin, J. Cao, W. Xu, Novel β-dicarbonyl derivatives as inhibitors of aminopeptidase N (APN), Bioorg. Med. Chem. Lett. 23 (2013) 4948–4952.
[22] L. Su, J. Cao, Y. Jia, X. Zhang, H. Fang, W. Xu, Development of synthetic aminopeptidase N/CD13 inhibitors to overcome cancer metastasis and angiogenesis, ACS Med. Chem. Lett. 3 (2012) 959–964.
[23] M. Drąg, J. Grembecka, M. Pawełczak, P. Kafarski, α-Aminoalkylphosphonates as a tool in experimental optimisation of P1 side chain shape of potential inhibitors in S1 pocket of leucine-and neutral aminopeptidases, Eur. J. Med. Chem. 40 (2005) 764–771.
[24] J. Jiao, H. Fang, X. Wang, P. Guan, Y. Yuan, W. Xu, Design, synthesis and preliminary biological evaluation of N-hydroxy-4-(3-phenylpropanamido) benzamide (HPPB) derivatives as novel histone deacetylase inhibitors, Eur. J. Med. Chem. 44 (2009) 4470–4476.
[25] F.K. Hansen, S.D.M. Sumanadasa, K. Stenzel, S. Duffy, S. Meister, L. Marek, R. Schmetter, K. Kuna, A. Hamacher, B. Mordmüller, M.U. Kassack, E.A. Winzeler, V.M. Avery, K.T. Andrews, T. Kurz, Discovery of HDAC inhibitors with potent activity against multiple malaria parasite life cycle stages, Eur. J. Med. Chem. 82 (2014) 204–213.
[26] R. Cincinelli, L. Musso, G. Giannini, V. Zuco, M. De Cesare, F. Zunino, S. Dallavalle, Influence of the adamantyl moiety on the activity of biphenylacrylohydroxamic acid-based HDAC inhibitors, Eur. J. Med. Chem. 79 (2014) 251–259.